IOP Publishing Semiconductor Science and Technology
Semicond. Sci. Technol. 34 (2019) 095003 (9pp) https://doi.org/10.1088/1361-6641/ab3071

# Characterization of inhomogeneous Ni/GaN Schottky diode with a modified log-normal distribution of barrier heights

**Noah Allen[1,3], Timothy Ciarkowski[2], Eric Carlson[2] and Louis Guido[1,2]**

[1] The Bradley Department of Electrical and Computer Engineering, Virginia Polytechnic Institute and State University, Blacksburg, VA 24060, United States of America
[2] Department of Material Science and Engineering, Virginia Polytechnic Institute and State University, Blacksburg, VA 24060, United States of America

E-mail: Noah.Allen@vt.edu

Received 18 March 2019, revised 28 May 2019
Accepted for publication 9 July 2019
Published 30 July 2019

**Abstract**

The current versus voltage (I-V) characteristics of a Ni/GaN Schottky diode are measured from 50 to 400 K and the temperature dependence of the extracted barrier heights and ideality factors is described as a consequence of lateral inhomogeneity at the metal-semiconductor (M-S) interface. It is shown that by invoking a modified log-normal distribution of barrier heights at the M-S interface, the extracted barrier height temperature dependence can be well explained. Further, it is shown that this approach can describe the voltage dependence of the lateral barrier distribution revealing that for effective barrier height values calculated at increasingly higher voltages, the distribution begins to converge on a single value of 0.77 eV. This value is in good agreement with the flat-band barrier height of 0.77 ± 0.02 eV extracted from capacitance-voltage (C-V) measurements on the same device. The same procedure is used to describe the parallel conduction path apparent at low temperatures, revealing its behavior is indicative of an additional Schottky region with an increased density of low barriers which are more heavily perturbed by external bias. Finally, the model is successfully applied to previously published work on various Schottky diodes structures.

Keywords: GaN, Schottky diode, barrier inhomogeneity, log-normal distribution, parallel conduction, I-V-T

(Some figures may appear in colour only in the online journal)

## 1. Introduction

Gallium nitride (GaN) has proven to be an excellent material to implement power semiconductor devices. This is largely because of its breakdown field strength, high-temperature performance, and the availability of conductive substrates so that vertical device topologies are possible. Fabricated Schottky barrier diodes (SBDs) can act as both a high frequency and low turn-on voltage rectifying device and as a means of quickly evaluating the semiconductor material quality. On GaN, however, the current-voltage (I-V) characteristics frequently deviate from ideal thermionic emission over a single barrier. These inconsistencies are typically attributed to a lateral variation in the barrier at the interface between the metal and semiconductor [1–5]. Carrier transport across this non-ideal interface has been analyzed with various models [6, 7] however, the continuous distribution model first discussed by Song *et al* [8] and formalized by Werner and Güttler [9] presents a method by which the interface inhomogeneity can be characterized by a probabilistic distribution without first having to make assumptions about the source of inhomogeneity. Ideally, if the cause of non-ideality can be

[3] Author to whom any correspondence should be addressed

 

accurately represented through these models, work can be done to link specific material growth and device fabrication methods to spurious electrical device behavior.

By first assuming that the fabrication of a real Schottky diode will have some lateral variation in the interfacial barrier height and that this variation takes the form of a Gaussian distribution, Werner and Güttler present a straight-forward method to determine the mean and standard deviation of said distribution. Then, assuming a bias dependence of the effective barrier height distribution, they show that voltage dependence of the mean and standard deviation cause experimentally extracted values of ideality factor larger than unity. The technique was developed further, using the same analysis method to describe interfaces with multiple non-interacting Gaussian distributions [10, 11] and then again using iterative solving techniques to describe interfaces with interacting Gaussian peaks [12]. Although these methods tend to provide agreement with experimental data, application to the sample presented in this work yielded results which did not fit the data or implied spurious behavior according to the underlying assumptions. It was found that instead of using a single or multi-Gaussian distribution model, a single modified log-normal distribution could be used. Additionally, work was done to understand the effect that voltage has on the barrier distribution, ultimately revealing that the modified log-normal distribution can be used to describe the interface as the diode approaches flat-band conditions. This process is then applied to the typically ignored low current parallel conduction path observed at low temperatures, revealing that it can be explained as stemming from a region of the M-S interface with a lower barrier and higher voltage dependence. Finally, the model is successfully applied to previously published data on $Pd_2Si$/p-Si [11], Au/p-GaTe [13] and Au/n-GaAs [14] Schottky diodes where a multi-Gaussian distribution model is utilized.

## 2. Inhomogeneous Schottky model

The current ($I$) induced across a Schottky barrier diode (SBD) according to thermionic emission theory for an applied voltage ($V_A$) is given by the following equation [15]:

$$I(V_A) = AA^*T^2 \exp\left(\frac{-q\phi_{b0}}{k_B T}\right)\left[\exp\left(\frac{q(V_A - IR_s)}{\eta k_B T}\right) - 1\right] \quad (1)$$

Where $A$ is the metal-semiconductor contact area, $A^*$ is the Richardson constant of GaN (26.4 $A/cm^2K^2$), $T$ is the temperature, $\phi_{b0}$ is the M-S interface barrier height at zero-bias, $\eta$ is the ideality factor, and $R_s$ is the series resistance. Werner and Güttler explain that the interface is likely not homogenous and perturbation due to surface roughness, metallic diffusion, and even dopant atom concentration abnormalities can create lateral variation in the barrier height [9]. The resulting I–V characteristics is thus a superposition of thermionic emission currents across an interface characterized by a distribution of barrier heights. Additionally, it is possible that the distribution itself is voltage dependent. The current-voltage relationship can be rewritten to include this distribution such that:

$$I(V_A) = AA^*T^2\left[\exp\left(\frac{q(V_A - IR_s)}{k_B T}\right) - 1\right] \times \int_{-\infty}^{\infty} P(\phi_b^V)\exp\left(\frac{-q\phi_b^V}{k_B T}\right)d\phi_b^V \quad (2)$$

Where $P(\phi_b^V)$ represents the voltage-dependent probability distribution of barrier heights apparent at the M-S interface and must satisfy,

$$\int_{-\infty}^{\infty} P(\phi_b^V)d\phi_b^V = 1 \quad (3)$$

A consequence of a laterally varying barrier height is both an additional temperature and voltage dependence of the I–V characteristics. Werner and Güttler [9] show that if thermionic emission over these regions is dominating, the resulting I–V characteristics will be indicative of a homogeneous barrier with this additional temperature and voltage dependence according to:

$$I(V_A) = AA^*T^2 \exp\left(\frac{-q\phi_b^{eff}(V, T)}{k_B T}\right) \times \left[\exp\left(\frac{q(V_A - IR_s)}{k_B T}\right) - 1\right] \quad (4)$$

Here, $\phi_b^{eff}(V, T)$ is the effective barrier height. For SBD's suffering from lateral inhomogeneity, values of zero-bias barrier height extracted from I–V measurements are considered equivalent to $\phi_b^{eff}(0, T)$. An expression of the effective barrier height dependence on the lateral barrier distribution can be found by setting equation (2) equal to (4).

$$\phi_b^{eff}(V, T) = -\frac{k_B T}{q}\ln\left(\int_{-\infty}^{\infty} P(\phi_b^V)\exp\left(\frac{-q\phi_b^V}{k_B T}\right)d\phi_b^V\right) \quad (5)$$

Typically, the ideality factor is used to indicate that the observed I–V characteristics deviate from pure thermionic emission. However, in the context of an M-S interface with an inhomogeneous barrier, the ideality factor quantifies the voltage dependence of the distribution. Again, assuming thermionic emission is the dominant current conduction mechanism and that the ideality factor itself is not voltage dependent, Werner and Güttler showed that the effective barrier height voltage dependence at a fixed temperature can be found by setting equation (1) equal to equation (4). This results in the following,

$$\phi_b^{eff}(V, T) = \left(1 - \frac{1}{\eta(T)}\right)\cdot V + \phi_{b0}(T) \quad (6)$$

Here $\phi_{b0}(T)$ and $\eta(T)$ are the values of zero-bias effective barrier height and ideality factor at the measurement temperature, $T$, from experimental I–V measurements, respectively. We can see that for SBD's with an ideality factor of 1, the effective barrier is voltage independent, otherwise it will increase linearly with the quantity $1 - 1/\eta(T)$. From

equations (5) and (6), work can be done to relate a proposed probability distribution and its voltage dependence to experimentally extracted values of effective barrier height and ideality factor, respectively.

Presuming the interface can be described by a single Gaussian distribution, Werner and Güttler show that the experimentally extracted values of effective barrier height and ideality factor from a range of temperatures can be plotted according to equations (14) and (17) in [9], respectively. This results in linear trends which can be fit to determine the Gaussian mean and standard deviation along with the voltage dependence of these parameters. Using the same process, Chand and Kumar [10, 11] showed that in cases where the effective barrier height and ideality factor plots yielded multiple regions of linearity, the lateral inhomogeneity can be described by multiple Gaussian distributions. However, for this to be true only one distribution should be active at each temperature range (non-overlapping distributions) and that data analysis will yield increasingly larger Gaussian means at higher temperatures. If experimental results do not follow this, Jiang *et al* [12] showed that the integral in equation (5) could be re-evaluated with a summation of Gaussian distributions and experimental data could be fit using sets of Gaussian mean, standard deviation and weighting factors as input parameters in an iterative solver.

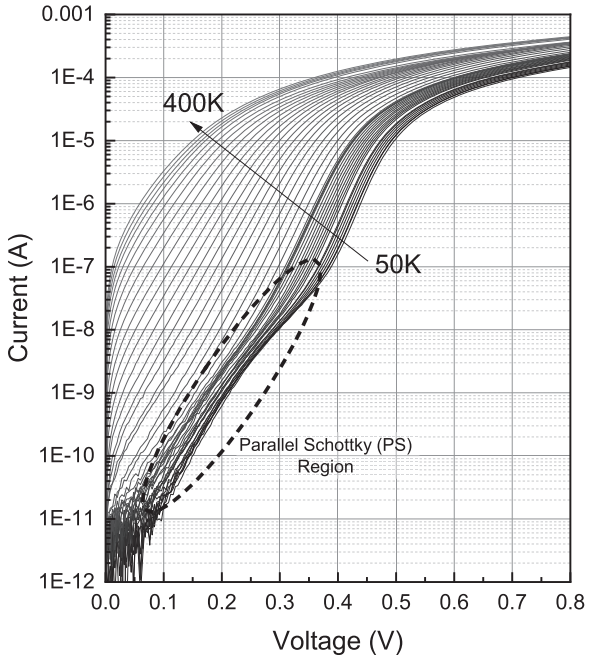


**Figure 1.** Measured forward bias current-voltage characteristics of the Ni/GaN Schottky diode from 50 to 400 K. The portion of the I–V characteristic measurement dominated by the low temperature parallel conduction is labeled 'Parallel Schottky (PS) Region'. (Note: I–V characteristics shown in increments of 8 K).

## 3. Experimental procedure

In this work we report experimental results of Schottky diodes fabricated on an n-type GaN film grown by MOCVD on sapphire. The film thickness is estimated at 1 $\mu$m and room-temperature capacitance versus voltage measurements indicate a free carrier concentration of $3 \times 10^{16}\,\mathrm{cm}^{-3}$. The sample was first sonicated in acetone then isopropyl alcohol for 10 min and rinsed in deionized water. Then a bath of aqua regia was used to remove metal ions from the surface of the sample followed by a 49% HF bath to remove any surface oxide layer, each sitting at room temperature for 10 min. Again the sample was rinsed in deionized water followed by a nitrogen drying step. Next, ohmic contact regions were defined via an optical lithography process, followed by a 1 min BOE dip to remove the native oxide layer. A Ti/Al/Ni/Ag (30/100/50/150 nm) metallization stack was deposited by E-beam and lift-off was performed in a solution of AZ400T photoresist stripper. The sample was annealed at 700 °C under a continuous flow of dry $N_2$ for 5 min to improve ohmic contact resistivity. Circular Schottky contact regions ranging in diameter from 73 to 250 $\mu$m were defined by optical lithography and a Ni/Ag (50/150 nm) stack was deposited by E-beam, yielding 128 diodes after lift-off. Barrier height and ideality factors were determined from room-temperature I–V measurements of each diode. The mean and standard deviation of extracted barrier heights across the sample was 0.74 and 0.04 eV respectively, while the extracted values of ideality factor were 1.09 and 0.12 respectively. Next, the sample was mounted to a temperature controlled stage in an MMR microprobe station with a CTI Model 22 cryostat where measurements were performed between 50 and 400 K in steps of 4 K on a characteristic 190 $\mu$m diameter diode. After temperature stabilized to within $\pm$100 mK of the target temperature for >30 s, the I–V characteristics of the reported device was measured by a Keithley 2400. C-V characteristics were recorded over the same temperature range using a DC sweep from 0 to −5 V and a 1 MHz probing signal from a SULA fast capacitance meter.

## 4. Results and discussion

The results of the I–V measurements taken at temperatures between 50 and 400 K are shown below in figure 1. As equation (1) predicts, when displayed on a semi-log plot each I–V measurement has a region of linearity characteristic of thermionic emission over a barrier followed by a roll-over at higher currents (>10 $\mu$A) due to series resistance. Additionally, measurements made at low temperatures (<256 K) exhibit two regions of linearity and roll-over indicative of a parallel conduction path. It is assumed this additional region stems from a Schottky interface with characteristics that don't allow it to dominate across the full temperature and voltage range, thus it is labeled the parallel Schottky (PS) region. One possible source of this phenomenon is a region with a voltage dependent barrier height which causes pinch off resulting in higher barrier regions to dominate as bias is increased. Later analysis will show that extracted values of ideality factor support this argument. In light of this additional region, equation (1) is modified to include the current contribution

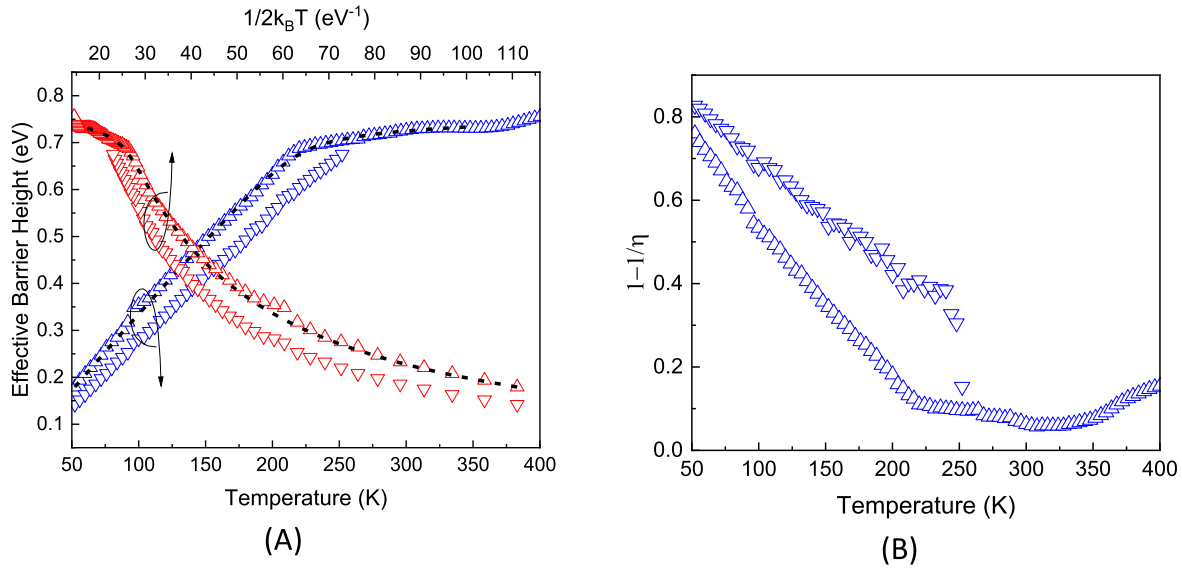


**Figure 2.** (A) Values for the effective barrier height extracted both from inside (∇) and outside (Δ) the PS region are plotted versus temperature and $1/2\boldsymbol{k_BT}$. The dashed line represents the best fit curves utilizing the modified log-normal distribution. (B) The extracted values of ideality factor at each temperature are plotted as $1 - 1/\boldsymbol{\eta(T)}$ according to equation (6).

from parallel SBD's at the same M-S interface.

$$I(V_A) = AA^*T^2\sum_{i=1}^{n}\exp\left(\frac{-q\phi_{b_i}^{eff}(0,T)}{k_BT}\right) \times\left[\exp\left(\frac{q(V_A - IR_{s_i})}{\eta_i k_BT}\right) - 1\right] \quad (7)$$

Here, the variables $\phi_{b_i}^{eff}(0, T)$, $\eta_i$, and $R_{si}$ are the zero-bias effective barrier height, ideality factor and series resistance of the *i*th SBD respectively. I–V data at each temperature is fit using a damped least-squares fitting procedure based on equation (7), where zero-bias effective barrier height, ideality factor and series resistance are passed as input parameters. In the case of the reported sample, $n$ is 2 for I–V measurements from 50 to 256 K, otherwise only one set of parameters was required and $n$ is 1. Fitting the full current versus voltage range produced values of $R^2 > 0.999$ for I–V measurements at each temperature. The zero-bias effective barrier height and ideality factor values which provide the best fit are plotted versus temperature in figures 2(A) and (B), respectively.

In both figures 2(A) and (B), parameters extracted from the PS region of the I–V curve are denoted by a downward triangle (∇) while all others are represented by an upward triangle (Δ). Extracted values of the effective barrier height were also plotted according to Werner and Güttler's single Gaussian distribution model, equation (14) in [9], shown as the red data points in figure 2(A). Reviewing the I–V curves, it is likely that at temperatures >350 K, extracted values of effective barrier height and ideality factor deviate from the actual value due to the dominance of series resistance. For this reason, values of effective barrier height and ideality factor extracted from I–V characteristics measure above 350 K were not used in subsequent fitting.

As discussed previously, if the interface is dominated by a single Gaussian distribution, plotting the effective barrier height versus $(2k_BT)^{-1}$ would linearize the data across the full temperature range however, this is clearly not the case. Because this deviation implies the interface cannot be represented by a single Gaussian distribution, the effective barrier height versus $(2k_BT)^{-1}$ data was fit with multiple lines. Fitting the barriers extracted from all but the PS region indicated the existence of three Gaussian distributions according to Chand and Kumar's method [10, 11]. However, calculated values of each distribution's mean did not increase monotonically with temperature and each of the distributions implied significant overlap thus violating the underlying assumptions. Finally, an attempt was made to fit the extracted barrier temperature dependence by iteratively varying the mean, standard deviation and weight of two Gaussian distributions following work done by Jiang *et al* [12]. Good agreement was found however, the results indicated that one of the distributions was characterized by a mean of 1.4 eV, a value larger than the theoretically predicted barrier height at a Ni/GaN interface (∼1.2 eV).

Broadly speaking, an arbitrary distribution of barrier heights could be used to fit the effective barrier height data according to equation (5) however, the dominance of lower barrier regions in the I–V relationship effectively hides contributions from higher barrier regions at the M-S interface. Unless inhomogeneity is minimal or measurements are taken at high enough temperature, values of effective barrier height indicative of the higher barrier regions will not be observed. Thus, the density of the unobserved barrier heights become imperceptible and a single optimal form of the distribution cannot be found. By constraining $P(\phi_b^V)$ with a defined probability density function, the form of the distribution outside of the observed range will be defined by the observed data and an optimal solution can be reached. In this work it was found that the range of effective barrier heights could be appropriately fit with a single modified log-normal

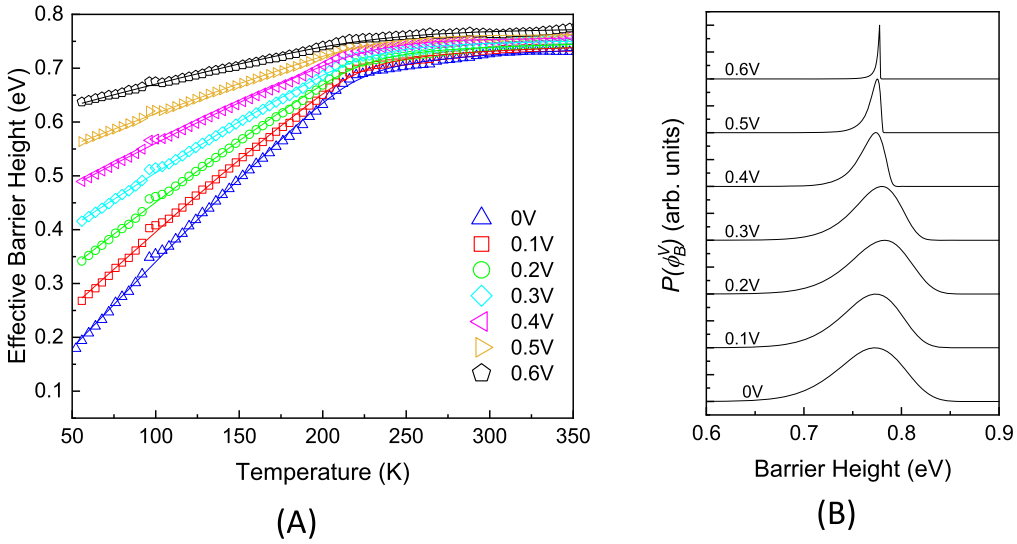


**Figure 3.** (A) The effective barrier height temperature dependence generated from extracted values of zero-bias effective barrier height and ideality factor according to equation (6) in steps of 100 mV from 0 to 600 mV (scatter). Fitting each set of data with the modified log-normal distribution resulted in the solid lines of best fit. (B) Normalized best fit probability function curves from the same voltage range.

distribution defined by equation (8) below.

$$P(\phi_b^V) = \frac{1}{C(-\phi_b^V + A)\sqrt{2\pi}} \times \exp\left(-\frac{[\ln(-\phi_b^V + A) - B]^2}{2C^2}\right) \quad (8)$$

Here $A$, $B$, and $C$ are used as input parameters to an iterative fitting routine that minimizes the error between generated effective barrier heights according to equation (5) and the experimentally determined values. In addition to these parameters, the lower limit of integration ($\phi_{LL}$) was used as an input to the fitting procedure while ensuring that equation (3) was met by scaling the resulting distribution on each iteration. This effectively estimates the form of the distribution at temperatures below what was measured however, instead of requiring the distribution to continue infinitely, even for negative values of effective barrier height, the distribution is weighted to zero below $\phi_{LL}$.

The fitting was first applied to effective barrier heights extracted from all but the PS region, represented with △ in figure 2(A), and the result is overlaid, shown as dashed lines. The good agreement with the experimental data indicates that a single modified log-normal distribution can be used to describe the inhomogeneous nature of the Ni/GaN SBD. The resultant fitting parameters $\phi_{LL}$,$A$, $B$, and $C$ used to fit the effective barrier heights extracted from all but the PS region are 11.5 meV, 0.94, −1.76 and 0.20 respectively.

With an appropriate probability density function established, the voltage dependence of the distribution can be examined. Continuing with the parameters extracted from all but the PS region, effective barrier height versus temperature plots are generated at incremental steps in voltage using equation (6) and extracted values of ideality factor. In figure 3(A), values of effective barrier height are calculated in steps of 100 mV from 0 to 600 mV, shown as scatter plots. Applying the modified log-normal fitting procedure at each bias step resulted in excellent agreement with the temperature dependent effective barrier height values (solid line). The resulting distributions of best fit are shown in figure 3(B) for each bias step.

Referring to the calculated set of effective barrier heights in figure 3(A), the data suggests that as the forward voltage is increased, regions at the M-S interface characteristic of lower effective barrier height (<0.65 eV) are strongly perturbed upward to higher values while those indicative of a higher effective barrier height are only slight perturbed as voltage is increased. Physically, this effect is consistent with the model proposed by Tung [6] where pinning at the M-S interface can induce a voltage-dependent conduction band saddle-point within the semiconductor. This saddle-point can become more strongly affected by voltage when the associated 'patch' is small and/or when strong pinning is present.

The resulting normalized best fit barrier distribution at each voltage step is shown in figure 3(B). In the plot we can see that as the voltage is increased, the distribution tails on both sides of the peak move toward each other and the form begins to converge to a prominent barrier value. On the low side of the distribution this is expected, assuming barrier 'pinch-off' is occurring however, this cannot explain the behavior of the distribution tail on the high side. As mentioned earlier, the temperature dependence of the effective barrier height is influenced more heavily by lower regions of barrier height according to equation (5). As the effective barrier height is generated at higher voltages, the trend begins to flatten out and the effect that lower barrier regions typically have is minimized. Thus, as the voltage is increased and the range of effective barrier heights begins to converge, the fitting procedure can more accurately represent the high side of the distribution. Comparing the barrier distribution at 600 mV with flat-band barrier heights extracted from C-V measurements, it becomes apparent that the value at which the

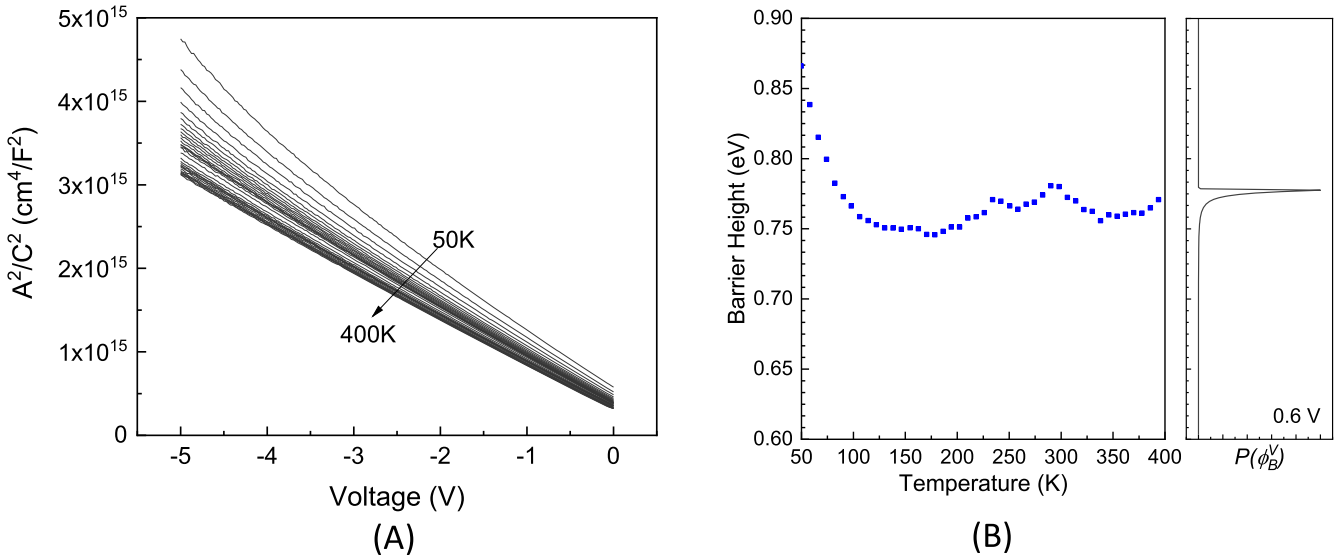


**Figure 4.** The (A) $A^2/C^2$ data calculated from C-V measurements and (B) the values of flat-band barrier height calculated at each temperature. The previously calculated barrier distribution at 0.6 V from I–V measurements is compared.

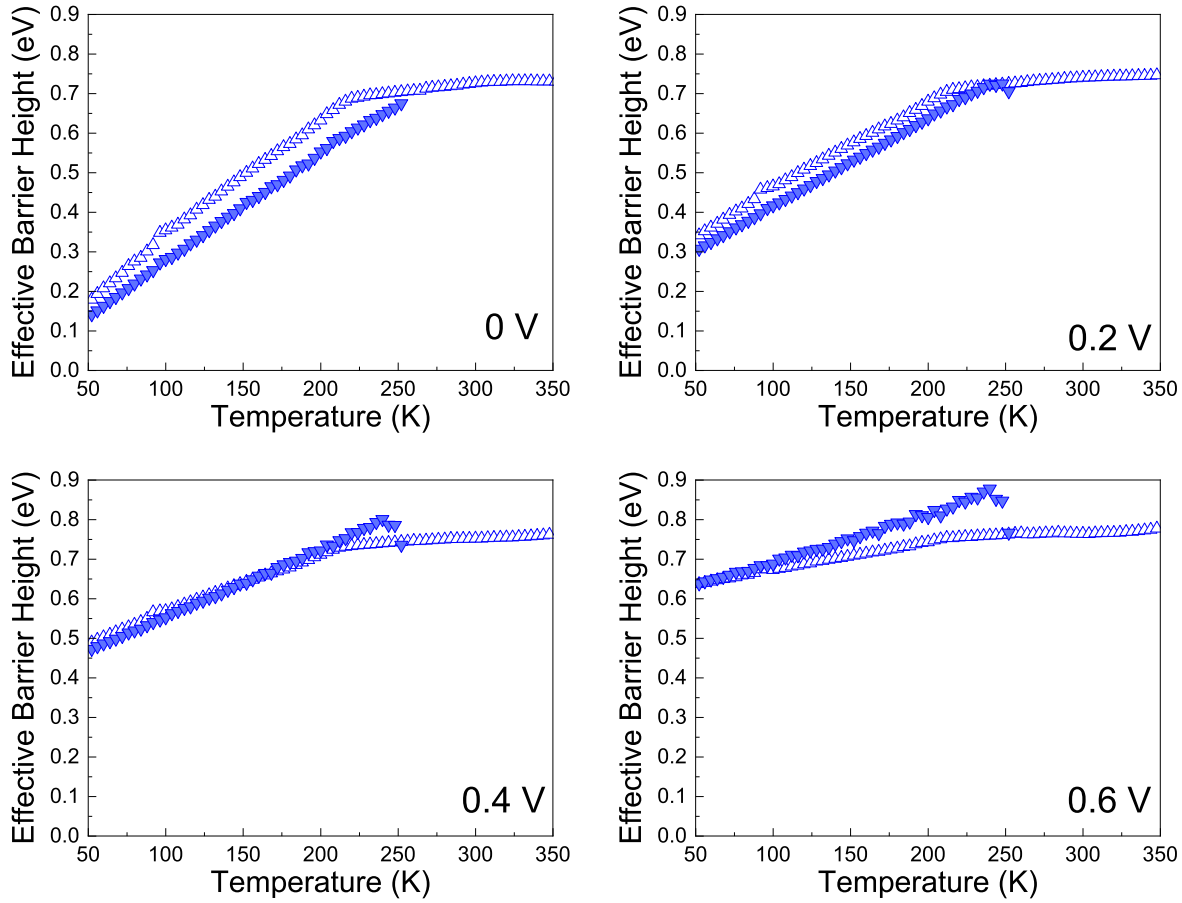


**Figure 5.** Effective barrier heights extracted from within (▼) and outside (△) the PS region of the I–V measurements calculated at 0, 0.2, 0.4, and 0.6 V according to equation (6).

probability distribution converges is the flat-band barrier height.

Capacitance versus voltage measurements were taken from 50–400 K in steps of 4 K from zero bias to −5 V. Below in figure 4(A), the measured capacitance versus voltage characteristics have been replotted to show the linear $A^2/C^2$ trends which are used to extract flat-band barrier height from the extrapolated value of the x-intercept according to

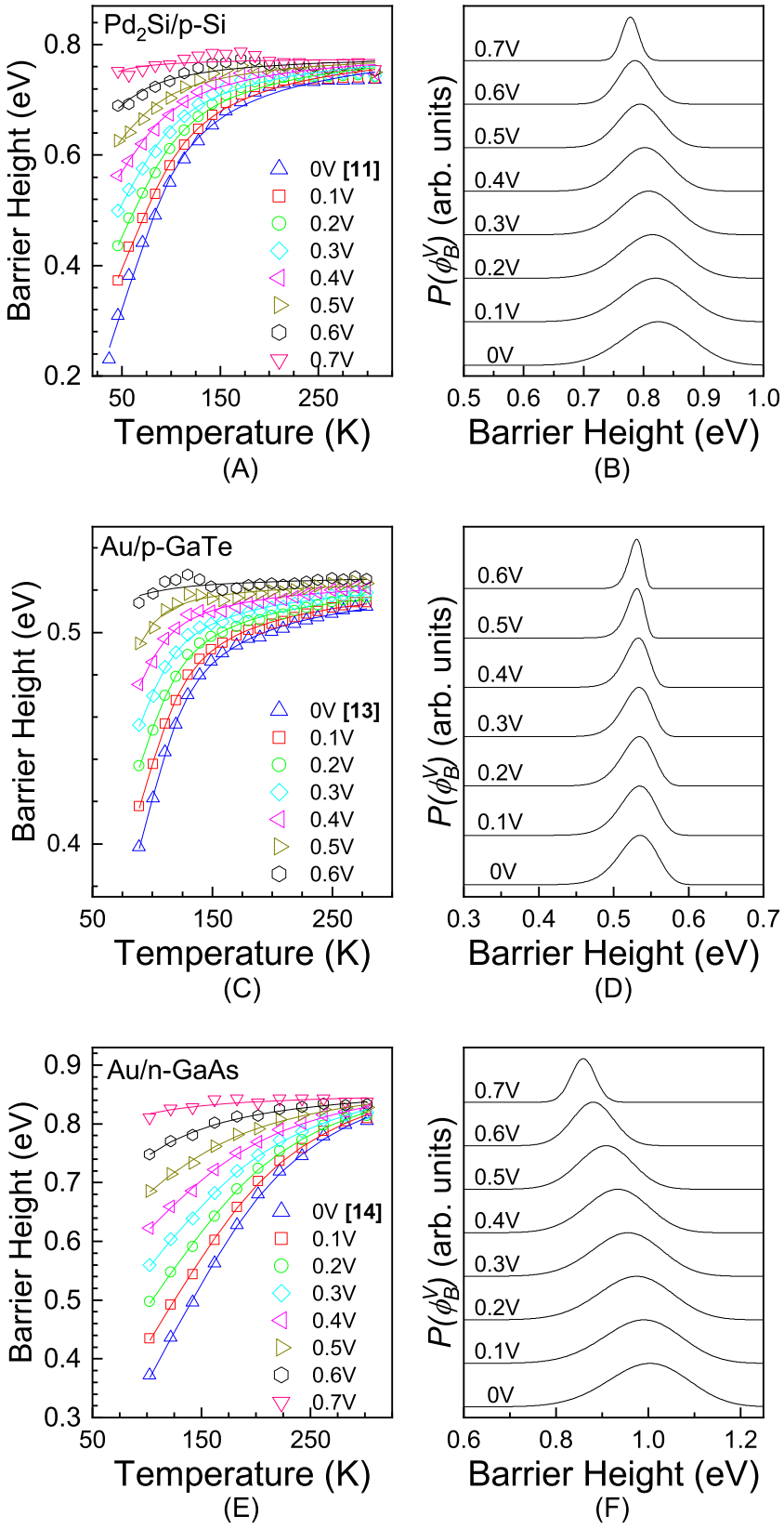


**Figure 6.** The modified log-normal model is applied to previously published data on (A) $Pd_2Si$/p-Si [11], (C) Au/p-GaTe [13], and (E) Au/n-GaAs [14] Schottky diodes (△). The scatter plot represents the temperature dependence of effective barrier heights calculated at increased forward bias. Fitting is shown as a solid line. Modified log-normal distributions calculated at each voltage are shown for the (B) $Pd_2Si$/p-Si, (D) Au/p-GaTe, and (F) Au/n-GaAs Schottky diodes.

equation (9).

$$\phi_b^{CV} = V_{FB} + \frac{k_B T}{q}\ln(N_C/N_D) + k_B T/q \tag{9}$$

$$N_D = \frac{-2}{q\varepsilon_r\varepsilon_0 \frac{d(A^2/C^2)}{dV}} \tag{10}$$

Here, $V_{FB}$ is the voltage required to induce flatband conditions and is equal to the extrapolated value of the x-intercept on the $A^2/C^2$ plot. $N_C$ is the temperature dependent conduction band density of states calculated from $4.3E14 \cdot T^{3/2}$, and the effective free carrier concentration , $N_D$, is calculated from the slope of the $A^2/C^2$ plot according to equation (10). The value $\varepsilon_r$ is the dielectric constant of GaN (8.9) and $\varepsilon_0$ is the permittivity in vacuum. Flat-band barrier heights calculated from the extrapolated values of $V_{FB}$ are shown in figure 4(B) versus temperature. On the right side of the graph, the barrier distribution calculated for effective barrier heights at 0.6 V is plotted for comparison. The effective barrier distribution peak occurs at 0.77 eV and the extracted values of flat-band barrier height are 0.77 ± 0.02 eV across the full temperature range. Good agreement between these two plots shows that the value at which the barrier distribution begins to converge is in fact the flat-band barrier height.

To understand the behavior of the PS region, the effective barrier heights were analyzed using the process outlined above. However, subsequent calculations of the effective barriers at increased voltages according to equation (6) had interesting effects. Figure 5 shows the evolution of the effective barriers extracted from the PS region (▼) as compared to those extracted from I–V characteristics outside of this region (△).

The zero-bias barriers extracted from the PS region (▼) increase with temperature until ∼250 K at which point the parallel conduction is no longer detectable in the I–V characteristics. Because the lower barrier region will dominate the I–V characteristics, it's theorized that the PS region disappears because the associated barrier height is the same as or larger than other areas at the M-S interface. When voltage is increased, as shown in the figure above, the effective barriers extracted from the PS region (▼) increases and as the trend moves upward, the point at which it crosses those extracted from outside the PS region (△) occurs at increasingly lower temperatures. Accordingly, this implies that the PS region within each I–V measurement should transition at lower voltages as the temperature is increased. Reviewing the I–V characteristics in figure 1, it can be seen that this is indeed the case. Similar to Tung's model [6], physically this effect could be caused by multiple patches at the M-S interface, each with characteristics that induce different voltage and temperature dependencies including size, pinning level and neighboring barrier properties.

## 5. Evaluation of previously published data

To relay the applicability of the modified log-normal approach for describing inhomogeneity in various Schottky diodes, previously published zero-bias effective barrier height and ideality factor data was evaluated using the procedure outlined above. In the selected published works, it was shown that the data is well described with a multi-Gaussian model however, reanalysis with the modified log-normal approach reveals that a single distribution can also explain the non-ideal I–V behavior. In figures 6(A), (C), and (E) the blue scatter (△) represents zero-bias effective barrier heights extracted from I–V measurements on $Pd_2Si$/p-Si [11], Au/p-GaTe [13] and Au/n-GaAs [14] Schottky diodes, respectively. Fitting these values with the modified log-normal distribution produces excellent agreement as shown by the blue line in each plot. The effective barrier height values at increased forward bias are calculated (scatter) according to equation (6), utilizing ideality factor data taken from each published work. Again, fitting the resulting data with the modified log-normal distribution (line) results in excellent agreement at each bias step for the reported Schottky diode data. Finally, the barrier height distribution which provided the best fit at each bias step is visualized in figures 6(B), (D), and (F) for the $Pd_2Si$/p-Si, Au/p-GaTe and Au/n-GaAs Schottky diodes, respectively.

Each of the previously published works relied on a multi-Gaussian distribution to analyze extracted effective barrier height and ideality factor data implying that the inhomogeneity in each of the three devices could be caused by more than one physical mechanisms at the interface. In reality, acceptable fitting of the effective barrier height temperature dependence relies more heavily on the distribution, $P(\phi_b^V)$, at lower magnitudes according to equation (5). Thus, it is possible that the usefulness of invoking a multi-Gaussian distributions comes from the ability to tailor the form of the distribution at lower magnitudes. With a single modified log-normal distribution, we show that the effective barrier height temperature dependence reported on $Pd_2Si$/p-Si [11], Au/p-GaTe [13] and Au/n-GaAs [14] Schottky diodes can accurately describe not only effective barrier height data at zero-bias but also at increasingly larger forward biases. Additionally, the model is further verified by the observation of distribution narrowing at increased bias which indicates that the Schottky diodes is approaching flat-band conditions.

## 6. Conclusion

In this work, we presented Ni/GaN Schottky diode I–V characteristics which could not be explained by the single Gaussian model proposed by Werner and Güttler [9]. Attempts to analyze the data with multi-Gaussian models proposed by Chand and Kumar [10, 11] or Jiang [12] yielded results which either violated underlying assumptions of the model or predicted impossibly large barrier height values for a Ni/GaN interface. To explain the temperature and voltage dependent effective barrier height behavior, a modified log-normal distribution is utilized and shows excellent agreement with experimental data. Next, it was found that subsequent calculations of the effective barrier height at increased voltages could be well explained using this distribution. Analysis

of the probability distribution at these voltages revealed that the trend begins to converge on a prominent barrier height (0.77 eV) which agrees well with that extrapolated from C-V measurements under flat-band conditions (0.77 ± .02 eV). Next, examination of the barriers extracted from the PS region of the I–V measurements reveal its behavior is indicative of an additional Schottky region characterized by a lower zero-bias effective barrier and stronger voltage dependence compared to those extracted outside of this region. Finally, the model was successfully applied to previously published data on $Pd_2Si$/p-Si [11], Au/p-GaTe [13] and Au/n-GaAs [14] Schottky diodes.

## Acknowledgments

The author would like to thank Virginia Tech's Bradley Research Fellowship for providing support for this work.

## ORCID iDs

Noah Allen https://orcid.org/0000-0002-9705-2709
Timothy Ciarkowski https://orcid.org/0000-0003-0989-6053
Eric Carlson https://orcid.org/0000-0001-5394-7052
Louis Guido https://orcid.org/0000-0002-5084-3626

## References

[1] Roccaforte F *et al* 2019 Barrier inhomogeneity in vertical Schottky diodes on free standing gallium nitride *Mater. Sci. Semicond. Process.* **94** 164–70
[2] Li X B *et al* 2019 GaN Schottky barrier diode with thermally stable nickel nitride electrode deposited by reactive sputtering *Mater. Sci. Semicond. Process.* **93** 1–5
[3] Yildirim N, Ejderha K and Turut A 2010 On temperature-dependent experimental I-V and C-V data of Ni/n-GaN Schottky contacts *J. Appl. Phys.* **108** 114506
[4] Dogan S, Duman S, Gurbulak B, Tuzemen S and Morkoc H 2009 Temperature variation of current-voltage characteristics of Au/Ni/n-GaN Schottky diodes *Physica E-Low-Dimensional Systems & Nanostructures* **41** 646–51
[5] Iucolano F, Roccaforte F, Giannazzo F and Raineri V 2007 Barrier inhomogeneity and electrical properties of Pt/GaN Schottky contacts *J. Appl. Phys.* **102** 113701
[6] Tung R T 1991 Electron-transport of inhomogeneous Schottky barriers *Appl. Phys. Lett.* **58** 2821–3
[7] Freeouf J L, Jackson T N, Laux S E and Woodall J M 1982 Effective barrier heights of mixed phase contacts—size effects *Appl. Phys. Lett.* **40** 634–6
[8] Song Y P, Vanmeirhaeghe R L, Laflere W H and Cardon F 1986 On the difference in apparent barrier height as obtained from capacitance-voltage and current-voltage-temperature measurements on Al/P-Inp Schottky barriers *Solid-State Electronics* **29** 633–8
[9] Werner J H and Guttler H H 1991 Barrier Inhomogeneities at Schottky Contacts *J. Appl. Phys.* **69** 1522–33
[10] Chand S and Kumar J 1996 Evidence for the double distribution of barrier heights in Pd2Si/n-Si Schottky diodes from I-V-T measurements *Semicond. Sci. Technol.* **11** 1203–8
[11] Chand S and Kumar J 1997 Electron transport and barrier inhomogeneities in palladium silicide Schottky diodes *Applied Physics a-Materials Science & Processing* **65** 497–503
[12] Jiang Y L, Ru G P, Lu F and Qu X P 2002 Schottky barrier height inhomogeneity of Ti/n-GaAs contact studied by the I-V-T technique *Chin. Phys. Lett.* **19** 553–6
[13] Gulnahar M and Efeoglu H 2009 Double barrier nature of Au/p-GaTe Schottky contact: linearization of Richardson plot *Solid-State Electronics* **53** 972–8
[14] Gullu O, Biber M, Duman S and Turut A 2007 Electrical characteristics of the hydrogen pre-annealed Au/n-GaAs Schottky barrier diodes as a function of temperature (in English)*Appl. Surf. Sci.* **253** 7246–53
[15] Rhoderick R H W E H 1988 *Metal-Semiconductor Contacts* 2nd edn (Oxford Science Publications)